J Biosci (2022)47:36
DOI: 10.1007/s12038-022-00264-9

Draft genome sequence and functional analysis of *Lysinibacillus xylanilyticus* t26, a plant growth-promoting bacterium isolated from *Capsicum chinense* rhizosphere

T A Phazna[1], Ng Ngashangva[1], Randhir Babu Singh Yentrembam[1], Ranjeet Maurya[2], Pulok Mukherjee[1], Chandradev Sharma[1], Praveen K Verma[2] and Indira Sarangthem[1]*

[1]*Microbial Resources Division, Institute of Bioresources and Sustainable Development (IBSD), Takyelpat, Imphal 795 001, India*

[2]*Plant Immunity Laboratory, National Institute of Plant Genome research (NIPGR), New Delhi 110 067, India*

**Corresponding author (Email, sidevi1@yahoo.co.in)*

MS received 10 October 2021; accepted 10 February 2022

Capsicum chinense is the chilli species containing the highest amount of capsaicin, and is an important traditional spice crop of Northeast India. Capsaicinoids derived from *C. chinense* are used in anticancer and anti-obesity treatments, as temperature regulators, in pain therapy, and as antioxidants. The current production and yield are very low due to the lack of organized cultivation and scientific inputs, and various plant diseases. Synthetic pesticides are frequently applied to boost yields, which creates potential risks to the environment, crops, and humans. The use of plant growth-promoting rhizobacteria is an alternative strategy in crop disease management to reduce the dependency on agrochemicals, which have detrimental effects on the environment. *Lysinibacillus xylanilyticus* t26 isolated from the *C. chinense* rhizosphere has shown good prospects in plant growth promotion and biocontrol. It showed strong antagonistic activity against *Pythium ultimum* ITCC 1650, *Rhizoctonia solani* ITCC 6491, and *Fusarium oxysporum* ITCC 6246. The draft genome sequencing of *L. xylanilyticus* t26 yielded a total of 5.69 Mbp with a G+C content of 36.80%. Genome analysis revealed that *L. xylanilyticus* t26 is very similar to *L. xylanilyticus* MH683160.1, and is phylogenetically related to *L. xylanilyticus* IBBPo7. Bioinformatics analysis predicted that it harbored type III polyketides, non-ribosomal peptides, terpenes, and lantibiotics including cerecidin, bacteriocins, siderophores, and thiopeptides, which are important traits of rhizobacteria for the utilization of minerals and to compete with other microbes for food. The strain t26 is a potential biocontrol agent for soil-borne fungal diseases. In this study, we derived the possible siderophore production pathways through the analysis of *L. xylanilyticus* t26 draft genome and plant growth response bioassays. The availability of genome data provides information that this draft genome harbored a siderophore BGC, which is 33% similar to petrobactin.

Keywords. Biocontrol; genome; *Lysinibacillus xylanilyticus*; rhizosphere; siderophore

1. Introduction

King chilli (*Capsicum chinense*) has broad-spectrum ethnopharmacological potential and is one of the most extensively grown spice crops of Northeast India (Meghvansi *et al.* 2010). The capsaicinoid compounds derived from *C. chinense* have uses in anticancer and anti-obesity treatments, temperature regulation, pain therapy, and as antioxidants (Meghvansi *et al.* 2010; Malangmeih *et al.* 2015). The quality and quantity of *C. chinense* are adversely affected by soil-borne and areal pathogens (Mathur *et al.* 2000; Sanatombi and

Supplementary Information: The online version contains supplementary material available at https://doi.org/10.1007/s12038-022-00264-9.

Published online: 22 June 2022

Sharma 2008). Production and yield are adversely affected by grey mold, fruit rot, leaf spot, blight, wilt, mottle virus, and black spot (Matthew *et al.* 2013). Therefore, synthetic pesticides are frequently applied to decimate pathogens and boost yields. However, this management strategy poses potential risks to the environment, soil microbiota, crops, and humans through bioaccumulation and bioamplification (Hyder *et al.* 2020).

The application of plant growth-promoting rhizobacteria (PGPR) is an alternative strategy to reduce dependency on agrochemicals in crop disease management, and its detrimental effects on the environment. PGPR are free-living or root-colonizing bacteria that confer plant growth promotion and do not cause harm to their hosts (Glick 2012). They competitively colonize roots and simultaneously act as biofertilizers for plants and as antagonists of pathogens (Kloepper and Schroth 1978). They promote plant growth through indole acetic acid (IAA) production (Etesami *et al.* 2015), phosphate solubilization, atmospheric nitrogen fixation, ACC deaminase activity, solubilization of inorganic mineral phosphates, and siderophore production (Beneduzi *et al.* 2012; Gupta *et al.* 2014). PGPR antagonizes soil pathogens by competing for resources such as iron, or by producing antimicrobials or lytic enzymes. They suppress plant pathogens by competition, siderophore production, antagonism, and induced systemic resistance (ISR), which activate multiple defense-related enzymes against phytopathogens (Vanitha and Umesha 2011).

A plethora of soil bacteria are considered PGPR, typically possessing more than one beneficial trait. PGPR exhibit biofertilization, rhizoremediation, stimulation of growth of roots, control of plant stresses, and reduction of plant diseases to augment plant growth (Lugtenberg and Kamilova 2009). Their biocontrol potential against phytopathogens and plant growth promotion (PGP) effects in major crops such as tomato, potato, cucumber, sugar beet, and cereals are well known. A large number of emblematic PGPR *Lysinibacillus* species have been characterized, unraveling the physiological and molecular basis of their PGP traits (Lee *et al.* 2010; Verma *et al.* 2014; Zhu *et al.* 2014). The systematic analysis of microbe genomes isolated from different types of soil using high-throughput sequencing technologies has served as a potent strategy to identify protein-coding sequences (CDS) contributing to PGP functions (Hayat *et al.* 2014; Burkett-Cadena *et al.* 2019; Ngashangva *et al.* 2021).

To the best of our knowledge, only four *L. xylanilyticus* genomes (*L. xylanilyticus* t26, *L. xylanilyticus* SR-84, *L. xylanilyticus* DSM, and *L. xylanilyticus* KCTC) have been deposited in the NCBI database at the time of writing. Despite its potential in agriculture and industry, limited information is available regarding its specific adaptations and mechanisms of biocontrol. Therefore, this study will give insights on strain t26 plant growth-promoting and biocontrol properties.

2. Materials and methods

2.1 *Isolation of rhizobacteria*

Soil samples were collected from rhizosphere soil of *C. chinense* grown in Manipur agro-ecological zones. The healthy root of *C. chinense* was placed in sterile distilled water and briefly vortexed and sonicated to remove soil aggregates and unwanted microbes (Bloemberg and Lugtenberg 2001). The turbid water was serially diluted and plated on Luria Bertania (LB) agar, Pikovskaya's Agar, Tryptic Soy (TSA) Agar, and Brain Heart Infusion (BHI) agar, and incubated at 30°C for 2–3 days. Morphologically distinct colonies were selected and subcultured repeatedly until pure culture colonies were obtained (Holt *et al.* 1994; Brock 1999). The isolated pure cultures were stored at 4°C until use.

2.2 *Screening of plant growth promotion and biocontrol activity*

The isolates were screened for PGP functions. The isolates that showed positive results were selected for testing using *C. chinense* seeds in an environmental growth chamber and under greenhouse conditions. PGP properties and environmental tolerance (pH, NaCl, Na_2CO_3, tolerance level) of strain t26 were evaluated (Wu *et al.* 2006). The phosphate solubilizing activity and protease activity of the isolated strains were tested on Pikovskaya's Agar and Skim Milk Agar (SMA), respectively (Hilda and Fraga 2000). The bacteria were inoculated with sterile toothpicks. For the positive strains, a halo zone was observed around the colonies after 5–7 days, and the solubilization index was expressed as follows (Nautiyal 1999):

$$(\text{colony diameter} + \text{halo zone diameter})/\text{colony diameter} \quad (1)$$

Chitinase activity was detected with the incorporation of colloidal chitin and indicator dye bromocresol purple in the media with a slight modification of the

Agrawal and Kotastha method (Agrawal and Kotastha 2009). The IAA production assay was carried out following the protocol of Bric *et al.* (1991) with some modifications. Briefly, bacterial strains were grown aerobically at 27°C with continuous shaking in rich nutrient broth supplemented with tryptophan. After 24 h, 3 mL from the culture's supernatant were transferred into 3 mL Salkowski reagent (0.5 M $FeCl_3$, 70% perchloric acid). The solution was vortexed and kept at room temperature for 30 min. The development of pink pigmentation was considered a positive reaction (Patten and Glick 1996). To measure IAA production, the optical density (OD) was recorded at 530 nm, and the IAA concentration was determined by comparison with the standard curve of different concentrations of IAA (ICN Pharmaceuticals, Cleveland, Ohio, USA) in the range 0.01–1 mM measured at 530 nm.

The nitrogen-fixing ability was tested using nitrogen-free media by stabbing the culture in the tube and incubating at 30±2°C for 4–5 days until the desired growth was observed along with the changing of media color to blue (Hartmann *et al.* 2006). The siderophore production was assayed by inoculating the bacterial isolates on Chrome Azurol S (CAS) Agar and incubating at 30±2°C for 4–5 days. The substrate color alteration from blue to orange and the formation of an orange circle (halo) around a single colony was considered a positive signal (Louden *et al.* 2011; García *et al.* 2012). The CAS medium was prepared using a modified protocol of Schwyn and Neilands (1987).

2.3 *Strain t26 antagonism bioassay*

The rhizobacteria of *C. chinense* were evaluated for their antagonistic activity against *P. ultimum* ITCC 1650, *R. solani* ITCC 6491, and *F. oxysporum* ITCC 6246. A 5 mm pathogen disc was inoculated at the center and the test PGPR was streaked on four sides with a gap of 3 cm approximately on potato dextrose agar (PDA) plates and incubated at 30±2°C for 2–3 days (Fokkema and Dickinson 1976). Plates inoculated only with the pathogen served as control. The inhibition percentage was calculated using the formula:

$$\text{Inhibition } \% = (\text{C} - \text{T})/\text{C} \times 100 \quad (2)$$

C represents the growth diameter of the pathogen in the control plate and T represents the pathogen diameter growth on the dual plate where both the test bacterial and the pathogen were placed (Okoli *et al.* 2008; Gunathilake *et al.* 2018).

2.4 *Genomic DNA isolation*

A single colony of t26 strain that exhibited maximum antagonistic activity was selected for genomic characterization. The genomic DNA (gDNA) of the pure culture pellet was lysed using Cetyl Trimethylammonium Bromide (CTAB) (Wilson 2001; Allen *et al.* 2006). The quality and quantity of the bacterial gDNA were determined by the A260/A280 ratio using an ultraviolet spectrophotometer (Nanodrop, Shimadzu Biotech Bio Spec-nano) and assessed using agarose gel electrophoresis (Song *et al.* 2012). The draft genome sequencing was performed through the Illumina HiSeq 2500 system (AgriGenome Labs (P) Ltd, Kerala) (Sahoo *et al.* 2019; Korostin *et al.* 2020).

2.5 *16S rRNA partial sequencing*

The internal transcribed spacer regions (ITS1 and ITS2) of the selected gDNA were amplified by polymerase chain reaction (PCR) using universal sense 16S rDNA primers 63F and 1387R. PCR conditions were 94°C for 5 min, followed by 30 cycles of 94°C for 1 min, 55°C for 1 min, and 72°C for 2 min, and final elongation at 72°C for 7 min (Marchesi *et al.* 1988). The PCR-amplified products were analyzed in 2% agarose gel in Tris-acetate (TAE) buffer (pH 7.9). The purified PCR products were sequenced in both directions, and sequences were assembled to create a final sequence (Saiki *et al.* 1988). A basic local alignment search tool (BLAST) analysis was performed to check the sequence similarities of the tested sequences with those sequences already deposited in the National Center for Biotechnology Information (NCBI) database (Camacho *et al.* 2009).

2.6 *Draft genome sequencing and assembly*

The crude gDNA was extracted from the overnight grown culture (Wilson, 2001; Sahoo *et al.* 2019). The genome sequencing was performed on the Illumina MiSeq/HiSeq (rapid) platform. Libraries were prepared with Illumina technology (Nextera XT DNA library preparation kit), and the adapter sequences were removed using Cutadapt version 1.8 (Martin 2011). The cleaned reads were subjected to the Kmer genie to predict the optimal *k*-value and assembly size (Chikhi and Medvedev 2014). *De novo* assembly was performed using SOAPdenovo2 (Luo *et al.* 2012). The tRNAscan-SE program was used for the detection of transfer RNA genes in genomic sequence (Lowe and Eddy, 1997). The

gene functional prediction was performed by Blast2GO against the databases (Conesa *et al.* 2005). The predicted genes were matched, with bacterial proteins from the Uniprot database, using the BLASTX program (Stephen *et al.* 2005; Camacho *et al.* 2009). Genes that could establish homology relationships (E-value $\leq 10^{-5}$ and similarity score $\geq 40\%$) were retained in the annotation pipeline while the others remain un-annotated.

2.7 *Genome annotation and functional characters*

The genome was annotated using NCBI PGAP v. 4.10 (Tatusova *et al.* 2016). Gene Ontology (GO) annotation was conducted using Blast2GO, which covered three domains: cellular component, molecular function, and biological process (Conesa *et al.* 2005). The genome features and comparative analyses were performed with the Joint Genome Institute—Integrated Microbial Genomes and Microbiomes (JGI-IMG), Kyoto Encyclopedia of Genes and Genomes (KEGG), and Rapid Annotation using Subsystem Technology (RAST) tools (Kanehisa *et al.* 2004; Overbeek *et al.* 2013). Function annotation of predicted open reading frames (ORFs) was performed based on a BLASTP search against NCBI non-redundant protein database and COG database (Stephen *et al.* 2005; Camacho *et al.* 2009; Tatusova *et al.* 2016).

2.8 *Global overview of* L. xylanilyticus *t26 genome*

The PGP functional traits of the t26 genome were analyzed using the database, JGI-M, and RAST tools (Kanehisa *et al.* 2004; Markowitz *et al.* 2010; Overbeek *et al.* 2013; Mukherjee *et al.* 2021), and the GO histogram was generated using WEGO4 (Web Gene Ontology Annotation Plot) (Ye *et al.* 2006). Integrated biochemical pathway maps were constructed based on analysis results of KEGG pathways (Kanehisa *et al.* 2016). The SEED-based classification assigned functional roles to the annotated genes that were then grouped into one or more subsystems (Overbeek *et al.* 2013). Annotation against the KEGG pathway classified the protein-coding genes into different pathway categories that may support plant growth (*www.kegg.jp/kegg/kegg1.html*) (Gupta *et al.* 2014; Kanehisa *et al.* 2016).

2.9 *Genome sequence comparison to determine close relatives*

A genome comparison of *L. xylanilyticus* t26 (NZ_PHQY01000000) was performed with its close relatives (Kanehisa *et al.* 2004, 2016; Brettin *et al.* 2015). A global alignment of *L. xylanilyticus* t26, *L. xylanilyticus* DSM23493, and *L. xylanilyticus* SR-86 nucleotides was performed using progressiveMauve and shown as local collinear blocks (LCBs) to find similarity among the genomes. Large-scale structural organization and evolutionary events such as structure and organization among the genomes were aligned using the Mauve software (Darling *et al.* 2004). The species similarity and common gene cluster shared among the related organisms were analyzed using Ortho Venn software (Wang *et al.* 2015). The presence of active microbial secondary metabolites (SMs) was analyzed with JGI-ABC using AntiSMASH v.5 software (Tilmann *et al.* 2015; Blin *et al.* 2019; Mukherjee *et al.* 2021).

2.10 *Phylogenetic analysis of* L. xylanilyticus *t26*

The 16s rDNA gene sequences of *L. xylanilyticus* t26 were aligned with publicly available *L. xylanilyticus* sequences from the NCBI database using the multiple sequence alignment method MUSCLE (Edgar 2004), and overhanging ends were trimmed in the software suite MEGA v6.06 (Tamura *et al.* 2013). All the retrieved and tested sequences were aligned using the ClustalW program and subjected to phylogenetic analysis. The phylogenetic tree was constructed using the neighbor-joining (NJ) method in MEGA6 with 1000 bootstrap replications and the evolutionary distances were calculated by using the Jukes–Cantor model (Tamura *et al.* 2013). Pairwise distances between all *L. xylanilyticus* strains were computed for both the 16S rDNA, and the NJ method was used to infer phylogeny from the observed pairwise distances (Saitou and Nei 1987). Bootstrap values were calculated with 1000 samples. A parsimonious phylogenetic network was constructed. Estimates of evolutionary divergence between sequences and the number of amino acid substitutions per site from between sequences are shown in figure 7. Analyses were conducted using the Poisson correction model. The analysis involved 12 amino acid sequences. All positions containing gaps and missing data were eliminated. There were a total of 594 positions in the final dataset.

3. Results

3.1 *PGPR and biocontrol activity screening*

The rhizobacteria were isolated from the rhizosphere soil of *C. chinense* roots. On the 3rd day,

morphologically distinct colonies were picked and subcultured repeatedly on LB agar to establish pure culture colonies. The strain t26 has shown potential plant growth promotion and disease control activity (table 1). It is a gram-positive, aerobic, motile, and rod-shaped bacterium. The strain t26 showed an inhibition zone (1.4 cm) on Pikovskaya's Agar, indicating its phosphate solubilizing activity, and it showed protease activity on SMA with an inhibition zone of 1.2 cm. Chitinase activity was detected with the incorporation of colloidal chitin and indicator dye bromocresol purple in the media. Its nitrogen-fixing ability was observed from the changing of the media color to blue. The siderophore production was assayed in the CAS medium by inoculating the bacterial isolates. The strain t26 exhibited antagonistic activity against *P. ultimum* ITCC 1650, *R. solani* ITCC 6491, and *F. oxysporum* ITCC 6246 (figure 1; table 1).

Table 1. The plant growth-promoting factors and disease control activities bioassay of t26 (inhibition zone diameters were measured in cm)

Plant growth-promoting factors (cm)								Antagonistic activity (cm)		
Protease	Cellulase	Glucanases	Chitinase	Phosphate solubilizing	Siderophore	Nitrogen fixation	IAA	Hydrogen cyanide	*P. ultimum*	*R. solani*	*F. oxysporum*
1.2	1.1	1.1	–	1.4	+	+	+++	++	1.0	1.1	0.9

3.2 *Genome sequencing and assembly of strain t26*

The draft genome was sequenced using 250 base pair (bp) paired-end reads on the Illumina HiSeq 2500 sequencing technology. The total number of raw reads (R1+R2) was 19,131,104 bp. The total number of base pairs was 4,782,780,000 bp with 37.73 GC% and a read length of 250. Cutadapt v1.8 was used to remove the data that may have contained adapter sequences (Martin 2011). All low-quality (Q<30) data were filtered out using sickle v1.33 (Joshi and Fass 2011). The reads of a length less than 30 bases were discarded and the duplicate reads were removed using FastUniq (Xu *et al.* 2012). The cleaned reads were subjected to Kmer genie (Chikhi and Medvedev 2014) to predict the optimal *k*-value and assembly size that was found to be 57 and 5311048 bp respectively. *De novo* assembly was performed using SOAPdenovo2 producing 769 contigs totaling 5,862,582 bp with N50 of 51,143 and L50 of 25 scaffolds and a GC content of 36.8% (Luo *et al.* 2012). SOAPdenovo2 assembly was used for all further downstream analyses (supplementary table 1). We predicted genes from the SOAPdenovo2 assembled contigs using Glimmer. We found 5952 predicted genes in the assembly. The clean reads produced a total length of 18,369,648 bp with 36.0 X fold coverage. The draft genome assembly contained 769 scaffolds and the largest contig was 407311bp with a G+C content of 36.80% (table 2).

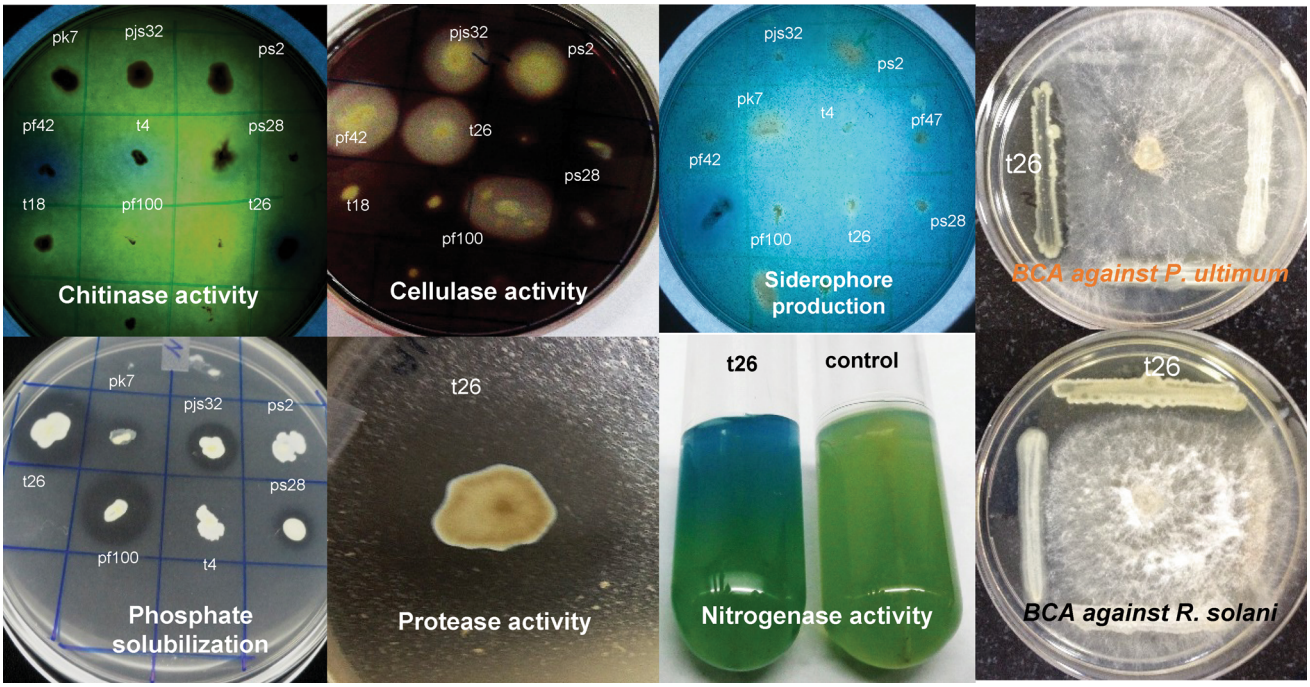

Figure 1. *In vitro* multiple plant growth promotion and biocontrol activity of t26. The test includes chitinase, cellulase, siderophore, BCAs, phosphate solubilization, protease, and nitrogenase activity of the rhizobacteria.

3.3 *Genome annotations*

The assembled draft genome sequence was annotated using NCBI Prokaryotic Genome Annotation Pipeline (PGAP) v.4.4, which identified 5956 genes, 5696 coding sequences (CDSs), 14, 38, 74 (5S, 16S, 23S) rRNAs, 13 (5S) complete rRNAs, 1, 38, 74 (5S, 16S, 23S) partial rRNAs, 130 tRNAs, and 4 non-coding RNAs (table 3). BLASTX searched against the Uniprot-bacteria database annotated 6045 genes. Around 80% of the genes could identify a homolog (E-value is 10^{-50}) which indicated high level of conservation of proteins. Around 96% of the predicted genes could identify a homolog with a similarity of more than 60% at the protein level with the existing proteins. A total of 127 rRNA operons comprising 14 5S rRNAs, 38 16S rRNA, and 75 23S rRNA genes together with 131 tRNA coding genes were predicted. In addition, 4 non-coding RNA genes and 199 pseudogenes were predicted in *L. xylanilyticus* t26 (table 3). The t26 genome is linear with a total length of 4,782,780,000 bp. Its closest species is *L. xylanilyticus* with a symmetrical identity of 74.4073%. Its closest genome is *L. xylanilyticus* DSM23493 with a symmetrical identity of 74.4073% (Tatusova *et al.* 2016).

The representative circular chromosome of *L. xylanilyticus* t26 was generated using GC View (figure 2). The data from this draft genome project was submitted to EMBL/GenBank/DDBJ databases under BioProjects: PRJNA419858, and BioSample: SAMN08100013, and the GenBank accession number NZ_PHQY01000000. The version described in this paper is version PHQY01000646.1. This strain has also been deposited in the MRC (Microbiology Repository Center), IBSD Microbial Culture Collection Centre under Accession no. I-10132387.

3.4 *Global overview of the genome for their functional characteristics*

The functional activity of carbohydrate metabolism, chemotaxis, cell motility, response to stress, metal ion binding, and oxidoreductase were predicted in *L. xylanilyticus* t26. They may directly or indirectly be involved in PGP and disease control activity. The KEGG pathway annotation classified the protein-coding genes into different pathway categories: metabolism, genetic information processing, environmental information processing, cellular processes, etc. Amino acid derivatives, carbohydrates, cofactors, vitamins, prosthetic groups, pigment, nucleosides, and nucleotides are the most abundant functional traits according to the KEGG annotations (*www.kegg.jp/kegg/kegg1.html*).

Four genomes of *L. xylanilyticus* strains isolated from different sources and locations are t26 from *C. chinensis* rhizosphere, India; strain DSM 23493T

Table 2. COG functions which are composed of 24 categories with 31.78% are of unknown function (annotation system: IMG (IMGAP v5.0.11) gene calling program: CRT 1.8.2)

Name	Count	Percentage
Amino acid transport and metabolism	468	8.97%
Carbohydrate transport and metabolism	200	3.83%
Cell cycle control, cell division, chromosome partitioning	67	1.28%
Cell motility	119	2.28%
Cell wall/membrane/envelope biogenesis	211	4.04%
Chromatin structure and dynamics	2	0.04%
Coenzyme transport and metabolism	249	4.77%
Defense mechanisms	155	2.97%
Energy production and conversion	238	4.56%
Extracellular structures	15	0.29%
Function unknown	414	7.94%
General function prediction only	565	10.83%
Inorganic ion transport and metabolism	330	6.33%
Intracellular trafficking, secretion, and vesicular transport	58	1.11%
Lipid transport and metabolism	214	4.1%
Mobilome: prophages, transposons	57	1.09%
Nucleotide transport and metabolism	140	2.68%
Posttranslational modification, protein turnover, chaperones	191	3.66%
Replication, recombination and repair	189	3.62%
Secondary metabolites biosynthesis, transport and catabolism	116	2.22%
Signal transduction mechanisms	328	6.29%
Transcription	500	9.58%
Translation, ribosomal structure and biogenesis	391	7.49%
Not in COG	2053	31.76%

(NZ_LFXJ01000000) isolated from forest humus, Korea (Liu *et al.* 2015); strain SR-86 (NZ_MDDN01000000) isolated from organic waste, Germany; and KCTC 13423 (SOEQ01000000) by DOE Joint Genome Institute (Loscar *et al.* 2016). The *L. xylanilyticus* t26 has the largest genomic size (5.68684 Mb) and the *L. xylanilyticus* SR-86 has the smallest genome size (4.76353 Mb). However, the GC % is comparatively similar at 36–37%, which indicates that they belong to the same species (table 3). The 661 ACGT tandem repeats identified in *L. xylanilyticus* t26 genome might play a variety of environmental regulatory and evolutionary roles. *L. xylanilyticus* t26 harbored a putative *trp* cluster gene (*trp*A, B, D, C, E, F, G) for tryptophan biosynthesis which may be involved in the biological processes of indole-3-acetic acid (IAA) and siderophore (petrobactin) biosynthesis. IAA is a primary plant hormone that regulates growth and development. The t26 genome encoded putative auxin efflux carrier proteins, suggesting its capability of producing and exporting IAA in a tryptophan-dependent manner.

3.5 *Functional analysis of the bacterial genome*

The WEGO annotation exhibited three different functions, viz. cellular component, molecular functions, and biological process. In the cellular component category, about 50% of the genes were involved in membrane composition and 40% of the genes were involved in cell composition. For the category of molecular function, binding, catalytic activity, and nucleic acid binding transcription factor activity were the top terms. Furthermore, the most abundant terms of the biological process are related to metabolic process (50%), regulation of biological process (8%), developmental process (3%), and molecular functions (about 9%) involved in cell transport activity (figures 3 and 4).

The metabolic process, cellular process, regulation of biological process, and biological regulation are among the top GO biological processes and molecular functions found in the strain t26 according to our WEGO analysis (figure 4). These terms are related to the functional class of genes that aid plant growth. A large number of genes are implicated in cell wall and capsule (12/48), amino acids and derivatives (8/48), membrane transport (5/8), protein metabolism (6/48), and DNA metabolism (4/8) that may help in plant growth (Gupta *et al.* 2014). KEGG pathway annotated 51.1% of the proteins and classified the protein-coding genes into different pathway categories, viz. carbohydrate metabolism, genetic information processing, environmental information processing, signaling, and cellular processes (*www.kegg.jp/kegg/kegg1.html*). The metabolism and environment information processing category pathways and unclassified protein (179) were highly represented, which indicated their unique characters (figure 4).

3.6 *Genome comparison of* L. xylanilyticus *t26 with its close relatives*

The GC content of the strain t26 is similar for *L. Lysinibacillus* SR-86 (36%) and *L. xylanilyticus* DSMZ 23493 (36.7%). The genome size of SR-86 is the smallest with approximately 4.8 Mbp compared with 5.6 Mbp of *L. xylanilyticus* t26. The 16S rDNA gene sequence of t26 exhibits the highest (100%) sequence similarity to *L. xylanilyticus* MH683160.1. The dot-

Table 3. Genomic features of the *L. xylanilyticus* and comparison with other *L. xylanilyticus* strains from the NCBI database

Genome description	*L. xylanilyticus* t26 (NZ_PHQY01000000)	*L. xylanilyticus* SR-86 (NZ_MDDN01000000)	*L. xylanilyticus* DSM 23493 (NZ_LFXJ01000000)	*L. xylanilyticus* KCTC 13423 (SOEQ01000000)	*L. sphaericus* OT4b.25 (NZ_CP014643)
Genomic size (Mb)	5.68684	4.76353	5.22164	5.17187	4.84166
Total protein count	5035	4474	4630	4866	4294
G+C content (%)	36.80	36.8	36.7	36.5	37.1436
CDS	5,783	4,633	4,630		4,565
Scaffolds	769	49	13	53	2
Total genes	6045	4743	4933	5199	4599
tRNA coding genes	131	74	99	68	107
rRNA coding genes	127	31	18	31	37
ncRNA genes	4	5	1	221	5
Pseudogenes	199	159	185		156
Genome coverage	36.0x	57.0x	150.0x	224.0x	97x

plot homology of synteny has shown that *L. xylanilyticus* t26 and *L. xylanilyticus* have discontinuous genomic variation, whereas the remaining genomes have high level of synteny. AntiSMASH v.5 has predicted 9 BGCs with high similarity to bacteriocin, siderophore (petrobactin 33%), betalactone (Fengycin 40%), terpene, TfuA-related, lanthipeptide (cerecidin 41%), thiopeptide, T3PKS, and bactericin (supplementary table 2). The predicted siderophore BGC region (gene bank file) was subjected to BLASTN and showed 92.85% similarity to *Lysinibacillus fusiformis* strain 1226 (Query coverage ~ 56% and E-value ~ 0.0) (Blin *et al.* 2019; Zhang *et al.* 2000). This siderophore BGC putative gene may be responsible for its PGPR characters (table 4).

3.7 *Siderophore and its putative biosynthesis pathway*

The regulatory logic of siderophore biosynthetic genes in bacteria involves the universal repressor Fur (Ferric Uptake Regulator), which acts together with iron as a negative regulator (Crosa and Walsh 2002). The siderophore biosynthetic pathway analysis of t26 with KEGG revealed that the isochorismate is converted into 2,3-dihydroxy benzoate with the help of isochorismatase. Isochorismatase is an intermediate for the synthesis of tryptophan, PAPA antibiotics, PABA, 3-hydroxyanthranilate, and more. The chorismate may have been derived from the biosynthesis of phenylalanine, tyrosine, and tryptophan (Jung *et al.* 2007) (figure 5).

Specifically, the siderophore is formed by the condensation of 3,4-dihydroxybenzoyl spermidine (3,4-DHB-SPD) with an activated form of citrate (coenzyme A or AMP ester) to form 3,4-dihydroxybenzoyl spermidinyl citrate (3,4-DHB-SPD-CT), followed by the condensation of a second 3,4-DHB-SPD subunit with 3,4-DHB-SPD-CT (again activated as coenzyme A or AMP ester) to form the mature siderophore (petrobactin) (table 5). A biosynthetic scheme for the assembly of petrobactin is analogous to the assembly of other siderophores including rhizobactin 1021, achromobactin, vibrioferrin, alcaligin, aerobactin, and desferrioxamine E (Jung *et al.* 2007). These data provided compelling evidence that AsbA may perform the penultimate step in the biosynthesis of petrobactin, involving condensation of 3,4-dihydroxybenzoyl spermidine with citrate to form 3,4-dihydroxybenzoyl spermidinyl citrate. As a final step, the data reveal that AsbB catalyzes the condensation of the second

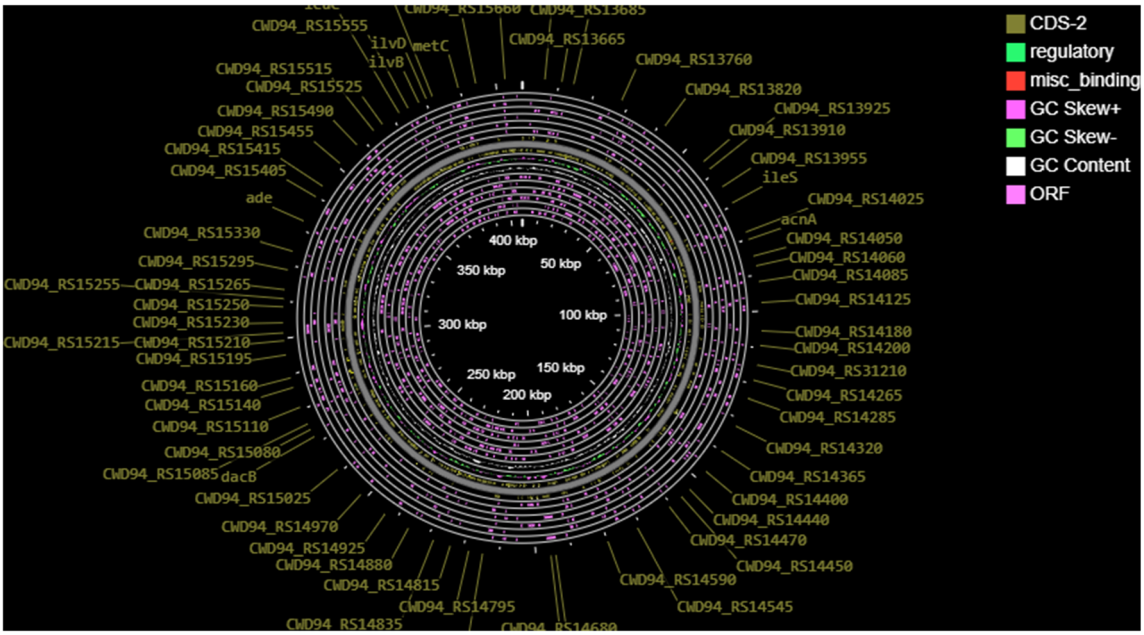

Figure 2. Circular genome map of *L. xylanilyticus* t26 generated using CG viewer (Jason and Paul 2008). The outer black circle represents the GC content; genome components such as ORFs, tRNA, rRNA genes, GC content, and CDS are listed against colored boxes.

molecule of 3,4-dihydroxybenzoyl spermidine with 3,4-dihydroxybenzoyl spermidinyl citrate to form the mature siderophore (figure 6).

3.8 *Phylogenetic analysis of* Lysinibacillus xylanilyticus *strain t26*

The analysis revealed that strain t26 is closely related to *Lysinibacillus xylanilyticus* strain IBBPo7. The strains *L. xylanilyticus* SE25, *L. xylanilyticus* GEM, *L. xylanilyticus* SYO3134, and *L. xylanilyticus* 12-2 formed a single clade (figure 7). The phylogenetic tree was generated in MEGA6 using the maximum-likelihood method with 1000 bootstrap replications. Numbers at each branch point correspond to the proportion of positive results from bootstrapping. The 16S rRNA sequence analysis of tested bacterial strains showed 98–100% identity with *Pseudomonas putida*, *P. libanensis*, *P. aeruginosa*, *Bacillus subtilis*, *B. megaterium*, and *B. cereus* sequences available in the NCBI GenBank nucleotide database.

3.9 *Genome-wide comparison and annotation of orthologous clusters*

The species, viz. *L. xylanilyticus* DSM23493, *L. xylanilyticus* SR-86, and *L. xylanilyticus* t26, that form 4302 clusters, 4207 orthologous clusters (at least containing two species), and 3148 single-copy gene clusters were compared. Among them, 3090 gene clusters are shared by the three organisms. Out of that, 27 gene clusters are unique to *L. xylanilyticus* t26 (figure 8). These 27 unique gene clusters may be involved in environmental adaptations and possibly SMs biosynthesis to compete with the other microbes. However, these assumptions need further experimental proof.

3.10 *Comparative genomics analyses of* L. xylanilyticus

Comparisons of genome structure for t26 vs. completely sequenced genomes of its closely related species, viz. *L. xylanilyticus* (*L. xylanilyticus* DSM23493 and *L. xylanilyticus* SR-86), are illustrated in figure 8. Each contiguously colored region is a locally collinear block (LCB), a region of homologous backbone sequence. LCBs below genome center lines are in reverse complement orientation relative to the reference genome. Lines between genomes trace each orthologous LCB through every genome. Large gray regions within the LCB signify the presence of lineage-specific sequences at that site; red lines represents uniqueness without any similarity to the other organism. The distribution of the genes among the *Lysinibacillus* genomes showed unique genes. The genome alignment

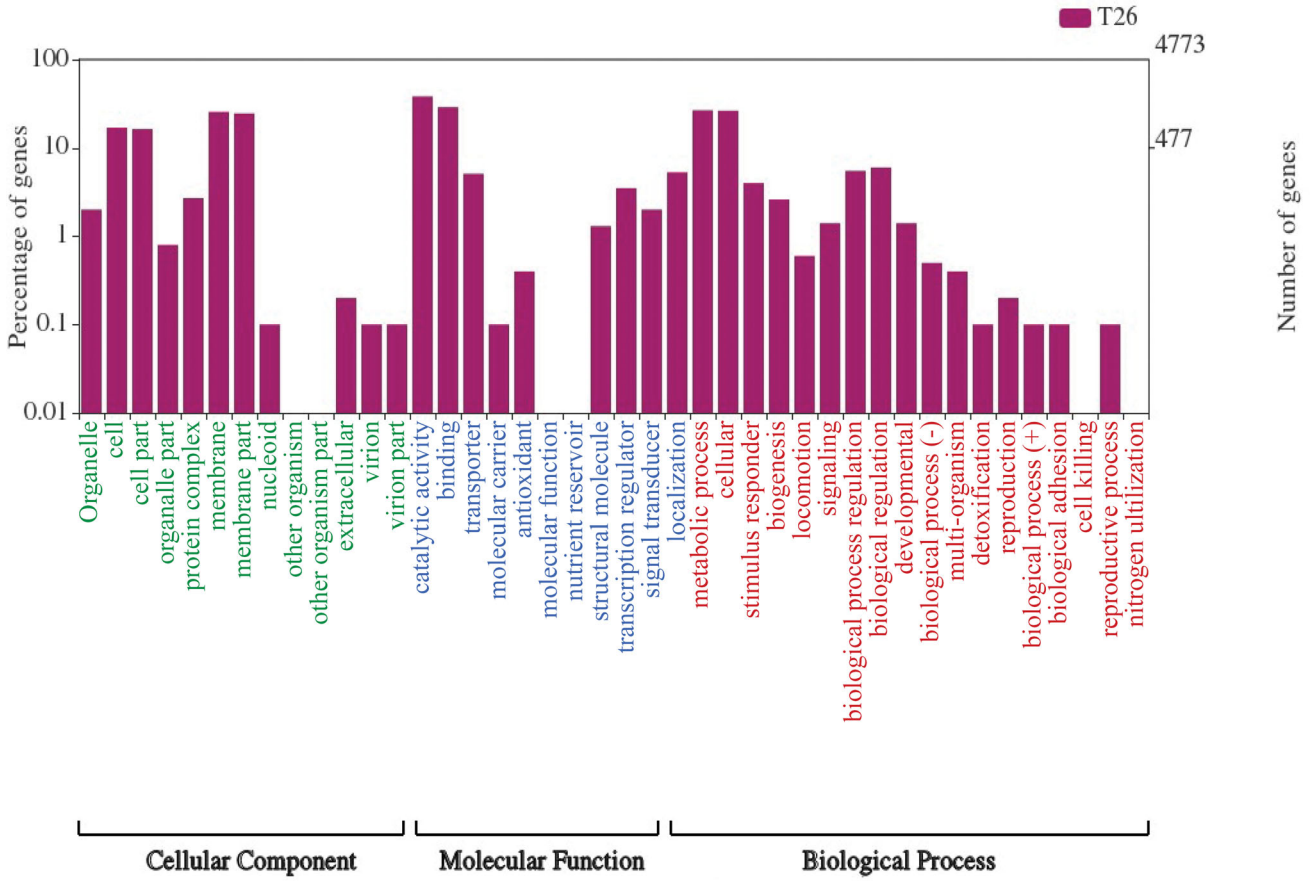

Figure 3. Traditional web gene ontology annotation histogram. The X-axis shows gene ontology terms and the Y-axis shows the percentages of genes (number of a particular gene divided by total gene number) (T26 – *Lysinibacillus xylanilyticus* t26).

showed extensive DNA rearrangement, as indicated by the blue lines, which is likely driven by the repeat sequences within the genome.

The nucleotide level similarity between DSM and SR-84 is markedly higher than the similarity between t26 strains (compare LCB composition between DSM, SR-84, and T26; figure 9), demonstrating a close relationship between these two strains. Furthermore, the close relationship between the chromosomes of DSM and SR-84 at the nucleotide level becomes evident, supporting the DSM and SR-84 strains forming a sub-clade within the *Lysinibacillus* species.

4. Discussion

In this study, we isolated the potential rhizobacteria strains associated with the local chilli cultivar. Thus, the identification and characterization of PGPR indigenous to chilli rhizospheres are important to screen bacterial isolates that can inhibit phytopathogens inoculum and enhance chilli growth (Lugtenberg and Kamilova 2009). We reported the draft genome sequencing and analysis of rhizobacteria strain t26 isolated from the roots of *C. chinense*. *C. chinense* is commonly cultivated in unorganized sectors mostly in the hill areas of Northeast India (Malangmeih *et al.* 2015). However, wastage remained very high (at least 20–30%) at different stages of cultivation, fruiting, harvest, and storage of *C. chinense*. These chilli are prone to soil-borne and areal pathogens (Mathur *et al.* 2000; Sanatombi and Sharma 2008; Matthew *et al.* 2013).

Nearly a thousand tons of fresh *C. chinense* are produced per annum in Northeast India and are preserved in dried and powdered form (Meghvansi *et al.* 2010). Nevertheless, this does not provide a stable price and income to the farmers due to its seasonal nature, diseases, storage issues, and low productivity. Because of the undesirable features of synthetic agrochemicals and the increasing threats to the environment, utilization of naturally occurring

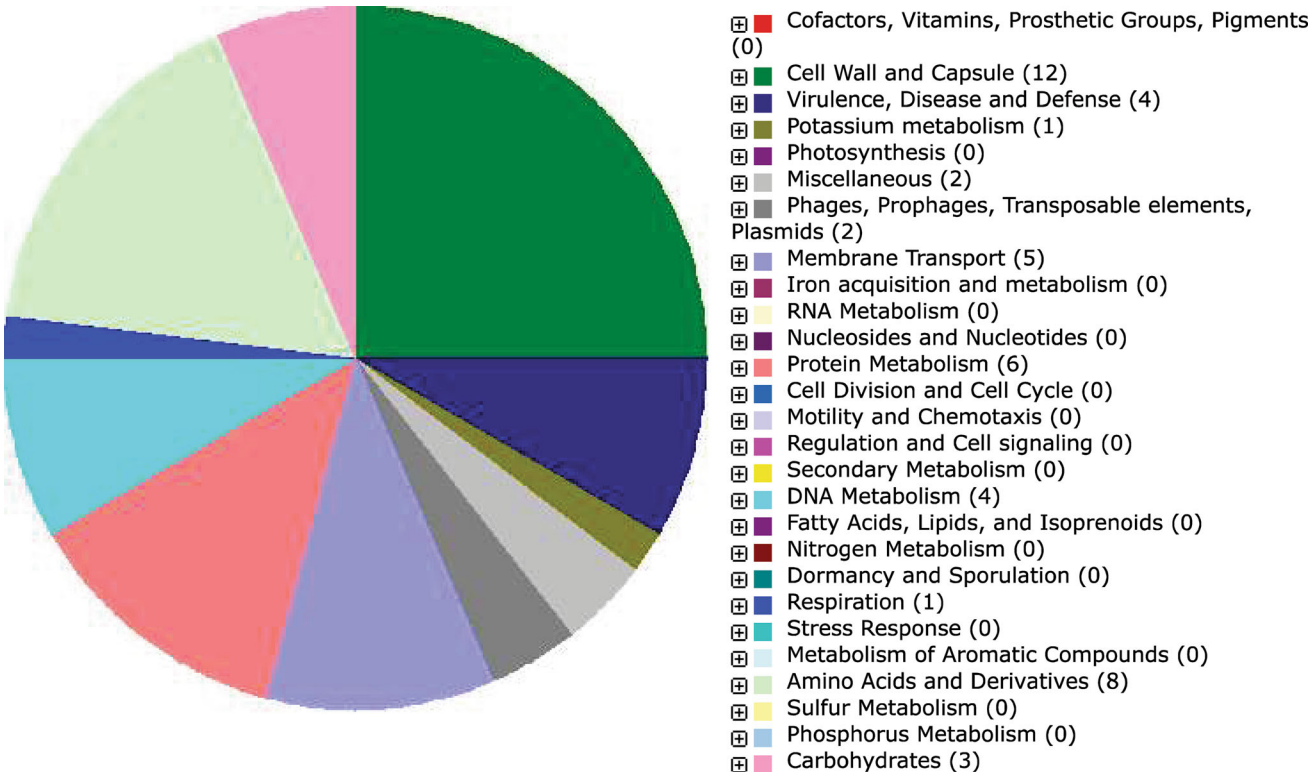

Figure 4. Functional traits identified from the whole genome sequence of t26 that were found connected with the KEEG pathway database. The figure was generated using the RAST annotation tool.

Table 4. BGC of siderophore (petrobactin) putative genes generated from AntiSMASH analysis

Sl. nos.	Protein	Protein ID	Locus tag
1	TetR/AcrR family transcriptional regulator	WP_100542260.1	CWD94_RS04610
2	GNAT family *N*-acetyltransferase	WP_100542261.12	CWD94_RS04615
3	Hypothetical protein	WP_100542262.1	CWD94_RS04620
4	Hypothetical protein	WP_100542263.1	CWD94_RS04625
5	Siderophore biosynthesis protein	WP_100542264.1	CWD94_RS04630
6	Siderophore biosynthesis protein	WP_100542265.1	CWD94_RS04635
7	AMP-binding protein	WP_100542266.1	CWD94_RS04640
8	Petrobactin biosynthesis protein AsbD	WP_049666019.1	CWD94_RS04645
9	Petrobactin biosynthesis protein AsbE	WP_100542267.1	CWD94_RS04650
10	Sugar phosphate isomerase/epimerase	WP_100542268.1	CWD94_RS04655
11	Hypothetical protein	WP_100542269.1	CWD94_RS04660

Figure 5. The BGC of the siderophore which is 33% similar to petrobactin. Gene clusters which are involved in the iron acquisition and metabolism through biosynthesis of the siderophore group of the non-ribosomal peptide pathway are centered on the focus gene (red color and numbered 5).

biological control agents for disease suppression and plant growth enhancement is sought as one of the possible alternatives. Non-judicious use of synthetic pesticides and fungicides has come under increasing public scrutiny in different countries, and pest resistance development is also increasing the menace for

Table 5. The putative enzymes of the petrobactin siderophore pathway derived from KEGG pathway database analysis

Sl. nos.	KO	Name	Definition	EC
1	K02552	menF	Menaquinone-specific isochorismate synthase	[EC:5.4.4.2]
2	K15652	asbF	3-Dehydroshikimate dehydratase	[EC:4.2.1.118]
3	K24108	asbA	Spermidine-citrate ligase	[EC:6.3.2.-]
4	K24109	asbB	3,4-Dihydroxybenzoyl-citryl-spermidine/N-citryl-spermidine-spermidine ligase	[EC:6.3.2.-]
5	K24110	asbC	3,4-Dihydroxybenzoate-[aryl-carrier protein] ligase	[EC:6.2.1.62]
6	K24112	asbE	Petrobactin synthase	[EC:2.-.-.-]

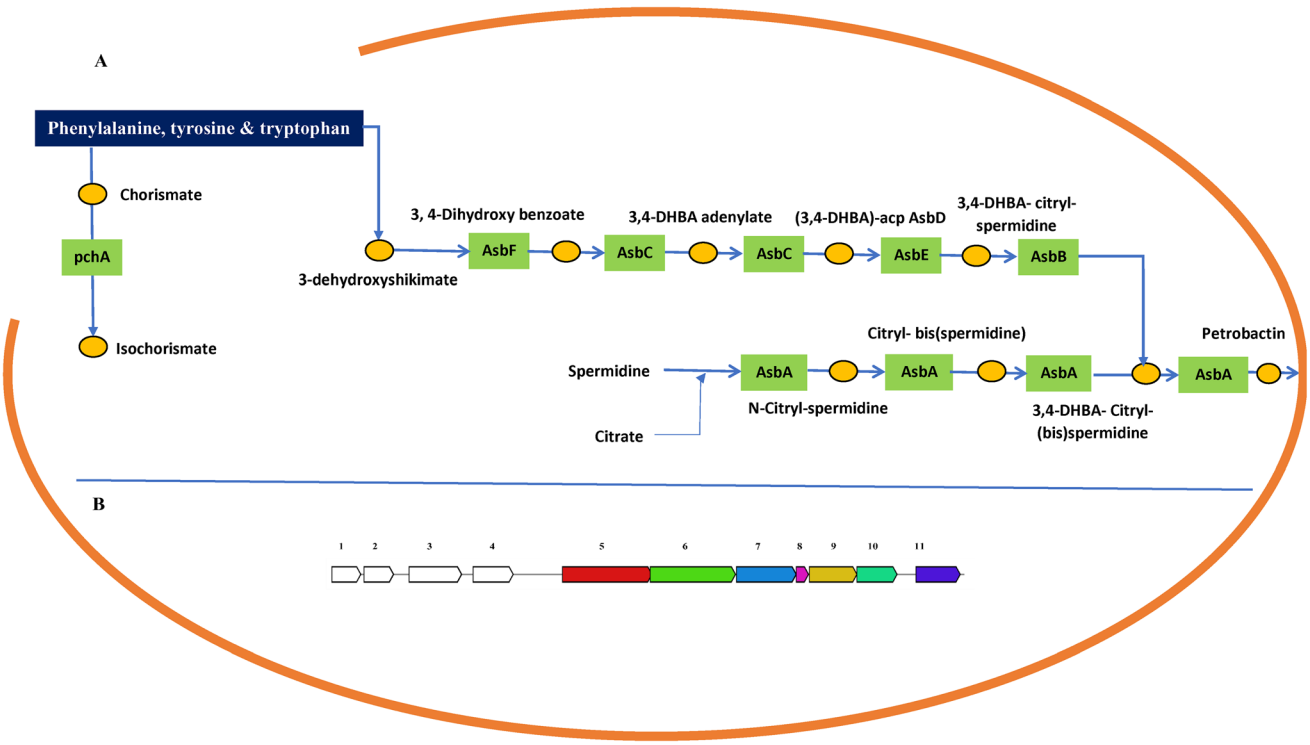

Figure 6. Biosynthesis pathway of siderophore (petrobactin) from *L. lysinibacillus* t26 predicted from KEGG Pathway analysis (green boxes indicate the putative enzymes of the pathway, the ochre dots indicate the intermediate biomolecules, and the circle represents the cell outline).

farmers. Furthermore, pesticides are noxious to the survival of beneficial rhizosphere microbes. Thus, there is a strong need to find cost-effective and environmentally safe alternatives which can minimize or eliminate the dependency on synthetic chemicals.

The microbial communities, or colonies, around the plant root system play an important role in maintaining proper growth, balancing nutritional requirements, and improving the health of the plant in varied conditions (Vessey 2003; Matthew *et al.* 2013). They act as biofertilizers and as antagonists (biopesticides) of root pathogens, including bacteria, fungi, and nematodes (Miguel and Clara 2003). They are applied to a wide range of agricultural plants to enhance growth and production, and for disease control. The bacteria associated with plant roots that exert beneficial effects on plant development are referred to as PGPR (Hardoim *et al.* 2008). PGPR is a potential natural alternative that can provide cross-protection against multiple stress factors and facilitate the growth of its symbiotic plant (Glick 2012). PGPR increase the fitness and growth of host plants through biological nitrogen fixation, synthesis of plant hormones, solubilization of inorganic mineral phosphates, and cellulose, protease, antibiotics, cyanide, and siderophore production (Beneduzi *et al.* 2012; Hyder *et al.* 2020).

Bacterial strains with strong antagonist potential were subjected to biochemical and molecular analysis. The combination of results from biochemical and taxonomical characterization led us to select the t26 strain. The bacterial strain t26 was tested for *in vitro* putative PGP traits, including IAA production, siderophore production, P-solubilization, and organic acid production. It is the first *L. xylanilyticus* strain of rhizobacteria isolated from *C. chinense* roots. The activity test of the strain has shown antagonism against *P. ultimum* ITCC 1650, *R. solani* ITCC 6491, and *F. oxysporum* ITCC 6246. The other biochemical activity test included protease, nitrogen-fixation, cellulase, chitinase, and siderophore activity (Fokkema and Dickinson 1976). It might also have exerted beneficial effects on growth promotion and biocontrol of the host plant (Bloemberg and Lugtenberg 2001; Verma *et al.* 2014).

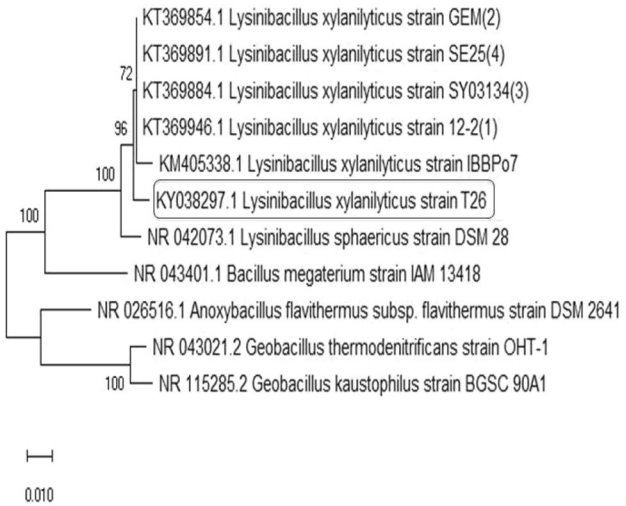

Figure 7. Phylogenetic tree highlighting the position of t26 relative to other type strains within the genus *Lysinibacillus*. The strains and other corresponding GenBank accession numbers of 16S rDNA genes are indicated in parentheses. The sequences were aligned using Clustal W and the neighbor-joining distance model by using MEGA6 bootstrap values determined from 1000 bootstrap replications.

The genomic-level characterization of PGPR from the roots of *C. chinense* indicated that the siderophore biosynthetic gene clusters were encoded by the t26 genome. It is 33% similar to petrobactin (Kanehisa *et al.* 2016). Siderophores are low-molecular-weight compounds with extremely high-affinity ferric iron chelators biosynthesized and excreted by most microorganisms that play an important role in iron acquisition (Köster, 2001; Brian *et al.* 2007). Siderophore-mediated scavenging of ferric iron from hosts contributes significantly to the virulence of pathogenic microbes. As a consequence, siderophore biosynthesis is an attractive target for chemotherapeutic intervention.

SEED-based classification analysis of the t26 strain proteins assigned functional roles to the annotated genes, and many of these siderophores are polypeptides that are biosynthetically derived from the non-ribosomal peptide synthetases (NRPS). The genome also

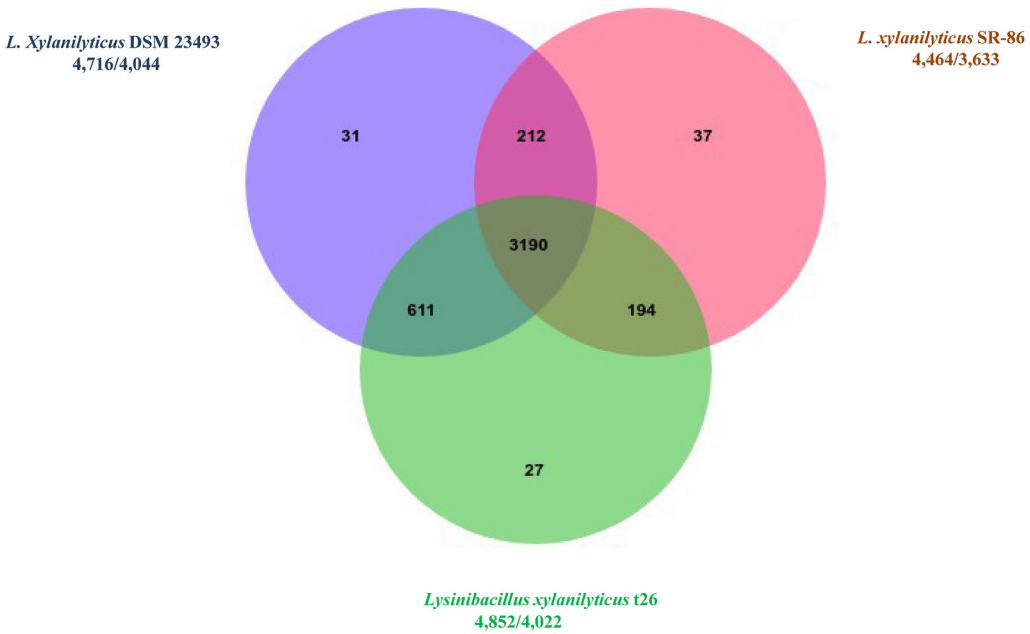

Figure 8. Venn diagram genome comparisons among the related species, i.e. annotated in the whole genome data in NCBI. viz., *L. xylanilyticus* DSM23493, *L. xylanilyticus* SR-86, and *L. xylanilyticus* t26.

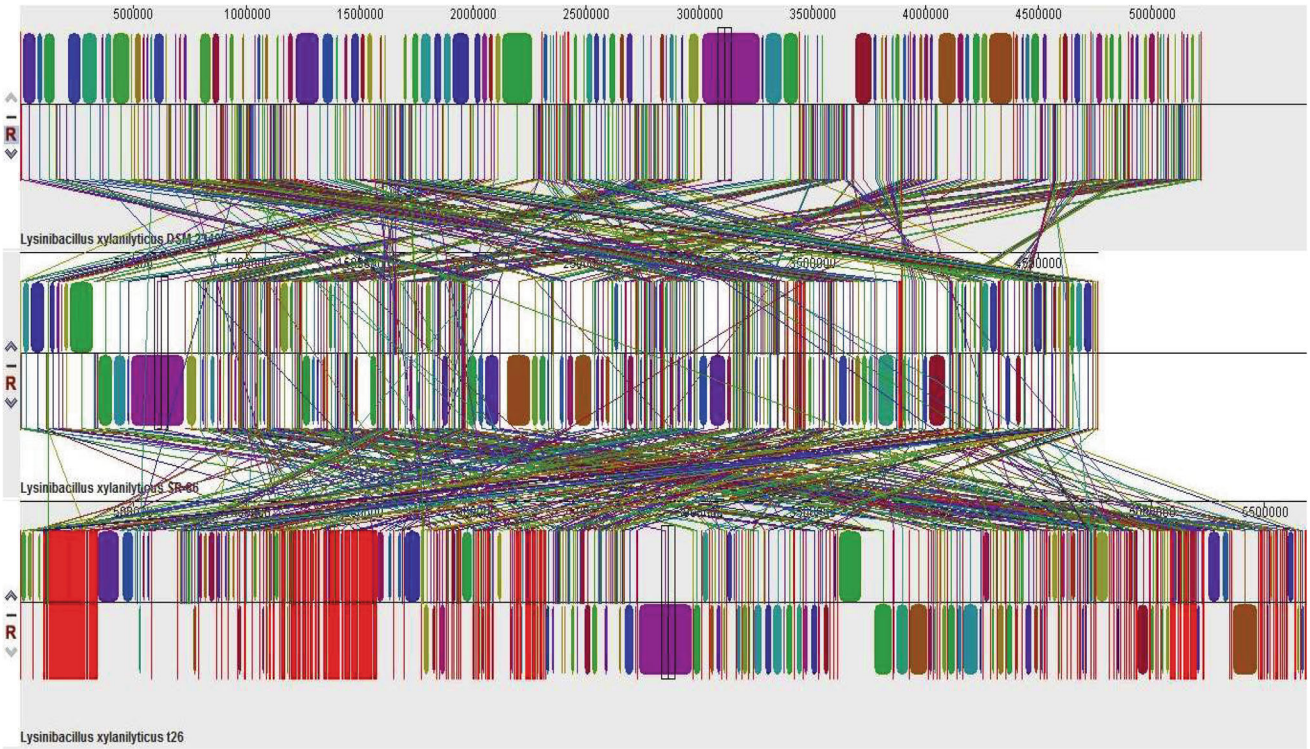

Figure 9. Comparative synteny line plots of the whole genome sequences of *L. xylanilyticus* t26, *L. xylanilyticus* DSM23493, and *L. xylanilyticus* SR-86. The analysis was carried out using the Artemis comparison tool and computed using TBLASTX with a cutoff E-value of 10^{-5}. The red bars between the DNA lines indicate individual TBLASTX matches, and the blue lines exhibit inverted matches.

Table 6. Proteins identified from t26 genomes by KEGG database analysis

KEGG	Gene name	Name
K00034	*gdh*	Glucose-1-dehydrogenase
K04750	*Phn B*	Phosphonate protein
K03781	*Kat E*	Catalase
K00432	*gpx*	Glutathione peroxidase
K04565	*SOD1*	Superoxide dismutase

encoded enzymes such as catalases, superoxide dismutases, and glutathione transferases, which are known to be involved in the management of oxidative stresses in plants (*www.kegg.jp/kegg/kegg1.html*). We identified putative genes encoding glucose-1-dehydrogenase (gdh; K00034) in the t26 genomes (table 6), suggesting that phosphate solubilization is likely mediated through gluconic acid secretion.

L. xylanilyticus t26 antagonistic activity and genome sequence analysis provide an in-depth understanding of the genome architecture of this species, thus facilitating future genetic engineering and applications in agriculture, industry, and medicine. Furthermore, this study highlights the current gap in our understanding of complex plant biomass metabolism in rhizosphere bacteria. PGPR exhibiting multiple traits may be used in the development of new, eco-friendly, and effective bio-formulations as an alternative to synthetic fungicides.

Author Contributions

SID, DS, and PKV conceived and designed the experiments. NN, PTA, and RMP wrote the paper. PTA, MP, CA, and CS isolated the genomic DNA from selected PGPR strains. Agri-genome Kerala performed the sequencing. NN, SID, and MP performed the analysis. SID, DS, and PKV provided technical advice, analysis support, and oversight.

Funding

This work was supported by the Department of Biotechnology, Government of India.

Competing interest The authors declared that they have no conflict of interest.

References

Agrawal T and Kotasthane AS 2009 A simple medium for screening chitinase activity of *Trichoderma* spp; in *Methods of molecular identification and laboratory protocols* (International Sub commission on *Trichoderma* and *Hypocrea* Taxonomy, ISTH)

Allen GC, Flores-Vergara MA, Krasynanski S, Kumar S and Thompson WF 2006 A modified protocol for rapid DNA isolation from plant tissues using cetyltrimethylammonium bromide. *Nat. Protoc.* **1** 2320–2325

Beneduzi A, Ambrosini A and Passaglia LMP 2012 Plant growth-promoting rhizobacteria (PGPR): their potential as antagonists and biocontrol agents. *Genet. Mol. Biol.* **54** 1044–1051

Blin K, Shaw S, Steinke K, *et al*. 2019 AntiSMASH 5.0: updates to the secondary metabolite genome mining pipeline. *Nucleic Acids Res.* **47** W81–W87

Bloemberg GV and Lugtenberg BJ 2001 Molecular basis of plant growth promotion and biocontrol by rhizobacteria. *Curr. Opin. Plant. Biol.* **4** 343–350

Brettin T, Davis JJ, Disz T, Edwards RA and Gerdes S 2015 RASTtk: a modular and extensible implementation of the RAST algorithm for building custom annotation pipelines and annotating batches of genomes. *Sci. Rep.* **5** 8365

Brian FP, Jung YL, Ravindranadh VS, *et al*. 2007 Characterization and analysis of early enzymes for petrobactin biosynthesis in *Bacillus anthracis*. *Biochemistry* **46** 4147–4157

Bric JM, Bostock RM and Silverstone SE 1991 Rapid *in situ* assay for indoleacetic acid production by bacteria immobilized on a nitrocellulose membrane. *Appl. Environ. Microbiol.* **57** 535–538

Brock TD 1999 *Milestones in microbiology 1546–1940,* 2nd editon (ASM Press) pp 215–218

Burkett-Cadena M, Sastoque L, Cadena J and Dunlap CA 2019 *Lysinibacillus capsici* sp. nov, isolated from the rhizosphere of a pepper plant. *Antonie Van Leeuwenhoek* **112** 1161–1167

Camacho C, Coulouris G, Avagyan V, *et al*. 2009 BLAST+: architecture and applications. *BMC Bioinfor.* **10** 421–430

Chikhi R and Medvedev P 2014 Informed and automated k-mer size selection for genome assembly. *Bioinformatics* **30** 31–37

Conesa A, Gotz S, Garcia-Gomez JM, *et al*. 2005 Blast2go: a universal tool for annotation, visualization and analysis in functional genomics research. *Bioinformatics* **21** 3674–3676

Crosa JH and Walsh CT 2002 Genetics and assembly line enzymology of siderophore biosynthesis in bacteria. *Microbiol. Mol. Biol. Rev.* **66** 223–249

Darling AC, Mau B, Blattner FR and Perna NT 2004 Mauve: multiple alignment of conserved genomic sequence with rearrangements. *Genom. Res.* **7** 1394–1403

Edgar RC 2004 MUSCLE: multiple sequence alignment with high accuracy and high throughput. *Nucleic Acids Res.* **32** 1792–1797

Etesami H, Alikhani HA and Hosseini HM 2015 Indole-3-acetic acid (IAA) production trait, a useful screening to select endophytic and rhizosphere competent bacteria for rice growth-promoting agents. *MethodsX* **2** 72–78

Fokkema JN and Dickinson T 1976 Antagonism between fungal saprophytes and pathogens on aerial plant; in *Microbiology of aerial plant surfaces* (Academic Press) pp 487–505

García CA, De Rossi BP, Alcaraz E, Vay C and Franco M 2012 Siderophores of *Stenotrophomonas maltophilia*: detection and determination of their chemical nature. *Rev. Argent. Microbiol.* **44** 150–154

Glick BR 2012 Plant growth-promoting bacteria: mechanisms and applications. *Scientifica* **2012** 963401

Gunathilake KDPP, Ranaweera KKDS and Rupasinghe HPV 2018 Influence of boiling, steaming and frying of selected leafy vegetables on the in vitro anti-inflammation associated biological activities. *Plants* **7** 22

Gupta A, Gopal M, Thomas GV, *et al*. 2014 Whole genome sequencing and analysis of plant growth-promoting bacteria isolated from the rhizosphere of plantation crops coconut, cocoa and arecanut. *PLoS One* **9** e104259

Hardoim PR, Van O, Verbeek LS, Van E and lsas JD, 2008 Properties of bacterialendophytes and their proposed role in plant growth. *Trends Microbiol.* **16** 463–471

Hartmann A, Baldani JI, Martin D, *et al.* 2006 *Proteobacteria alpha and beta subclasses. The Prokaryotes V* (Springer Verlag, New York, USA) pp 115–140

Hayat R, Ahmed I, Paek J, *et al*. 2014 *Lysinibacillus composti* sp. nov., isolated from compost. *Ann. Microbiol.* **64** 1081–1088

Hilda R and Fraga R 2000 Phosphate solubilizing bacteria and their role in plant growth promotion. *Biotech. Adv.* **17** 319–359

Holt JG, Krieg NR, Sneath PHA, Staley JT and Williams ST 1994 *Bergey's manual of determinative bacteriology,* 9th edition (Lippincott Williams & Wilkins)

Hyder S, Gondal AS, Rizvi ZF, *et al*. 2020 Characterization of native plant growth-promoting rhizobacteria and their anti-oomycete potential against Phytophthora capsici affecting chilli pepper (*Capsicum annum* L.). *Sci. Rep.* **10** 3859

Jason RG and Paul S 2008 The CGView Server: a comparative genomics tool for circular genomes. *Nucleic Acids Res.* **36** W181–W184

Joshi N and Fass J 2011 Sickle: A sliding-window, adaptive, quality-based trimming tool for FastQ files (Version 1.33)

Jung YL, Brian KJ, Karla DP, *et al*. 2007 Biosynthetic analysis of the petrobactin siderophore pathway from *Bacillus anthracis*. *J. Bacteriol.* **189** 1698–1710

Kanehisa M, Goto S, Kawashima S, Okuno Y and Hattori M 2004 The KEGG resource for deciphering the genome. *Nucleic Acids Res.* **32** D277–D280

Kanehisa M, Sato Y and Morishima K 2016 BlastKOALA and GhostKOALA: KEGG tools for functional characterization of genome and metagenome sequences. *J. Mol. Biol.* **428** 726–731

Kloepper JW and Schroth MN 1978 Plant growth-promoting rhizobacteria on radishes. 4th Int. Conf. Plant Pathogenic Bacter Station de Pathologie Vegetale et Phytobacteriologie, INRA, Angers, France. pp 879–882

Korostin D, Kulemin N, Naumov V, *et al*. 2020 Comparative analysis of novel MGISEQ-2000 sequencing platform vs Illumina HiSeq 2500 for whole-genome sequencing. *PLoS One* **15** e0230301

Köster W 2001 ABC transporter-mediated uptake of iron, siderophores, heme and vitamin B12. *Res. Microbiol.* **152** 291–301

Lee CS, Jung YT, Park S, Oh TK and Yoon JH 2010 *Lysinibacillus xylanilyticus* sp. nov., a xylan-degrading bacterium isolated from forest humus. *Int. J. Syst. Evol. Microbiol.* **60** 281–286

Liu GH, Liu B, Wang JP, Che JM and Zheng XF 2015 Draft genome sequence of type strain *Lysinibacillus xylanilyticus* DSM 23493T. *Gen. Announc.* **3** 5

Loscar ME, Huptas C, Wenning M, Sieber V and Schmida J 2016 Draft genome sequence of *Lysinibacillus xylanilyticus* SR-86. *Gen. Announc.* **4** 6

Louden BC, Haarmann D and Lynne AM 2011 Use of blue agar CAS assay for siderophore detection. *J. Microbiol. Biol. Educ.* **12** 51

Lowe TM and Eddy SR 1997 tRNAscan-SE: a program for improved detection of transfer RNA genes in genomic sequence. *Nucleic Acids Res.* **25** 955–964

Lugtenberg B and Kamilova F 2009 Plant-growth-promoting rhizobacteria. *Annu. Rev. Microbiol.* **63** 541–556

Luo R, Liu B, Xie Y, Li Z and Huang W 2012 SOAP denovo 2: an empirically improved memory-efficient short-read de novo assembler. *Gigascience* **1** 18

Malangmeih L, Dey G and Sagolsem S 2015 Rural livelihood system in Manipur with special reference to cultivation of king chilli L. *J. Crop Weed.* **11** 144–151

Marchesi JR, Sato T, Weightman AJ, *et al*. 1998 Design and evaluation of useful bacterium-specific PCR primers that amplify genes coding for bacterial 16S rRNA. *Appl. Environ. Microbiol.* **64** 795–799

Markowitz VM, Chen IM, Palaniappan K, *et al*. 2010 The integrated microbial genomes system: an expanding comparative analysis resource. *Nucleic Acids Res.* **38** D382–D390

Martin M 2011 Cutadapt removes adapter sequences from high-throughput sequencing reads. *Embnet J.* **17** 10–17

Mathur R, Dangi RS, Dass SC and Malhotra RC 2000 The hottest chilli variety in India. *Curr. Sci.* **79** 287–288

Matthew GB, Lindsey O-H, Lange AJ, James MB and Linda LK 2013 Plant monocultures produce more antagonistic soil *Streptomyces* communities than high-diversity plant communities. *Soil Biol. Biochem.* **65** 304e312

Meghvansi MK, Siddiqui S, Khan MH, *et al*. 2010 Naga chilli: a potential source of capsaicinoids with broad-spectrum ethnopharmacological applications. *J. Ethnopharmacol.* **132** 1–14

Miguel AA and Clara IN 2003 Soil fertility management and insect pests: harmonizing soil and plant health in agroecosystems. *Soil Tillage Res.* **72** 203–211

Mukherjee S, Stamatis D, Bertsch J, *et al*. 2021 Genomes online database (GOLD) vol 8: overview and updates. *Nucleic Acids Res.* **49** D723–D733

Nautiyal CS 1999 An efficient microbiological growth medium for screening phosphate solubilizing microorganisms. *FEMS Microbiol. Lett.* **170** 265–270

Ngashangva N, Mukherjee P, Sharma KC, Kalita MC and Indira S 2021 Analysis of antimicrobial peptide metabolome of bacterial endophyte isolated From traditionally used medicinal plant *Millettia pachycarpa* Benth. *Front. Microbiol.* **12** 656896

Okoli CO, Akah PA, Onuoha NJ, *et al*. 2008 *Acanthus montanus*: an experimental evaluation of the antimicrobial, anti-inflammatory and immunological properties of a traditional remedy for furuncles. *BMC Complement. Altern. Med.* **8** 27

Overbeek R, Olson R, Pusch GD, *et al*. 2013 The SEED and the rapid annotation of microbial genomes using subsystems technology (RAST). *Nucleic Acids Res.* **42** D206–D214

Patten CL and Glick BR 1996 Bacterial biosynthesis of indole-3-acetic acid. *Can. J. Microbiol.* **42** 207–220

Sahoo D, Devi N, Ngashangva N, *et al*. 2019 Draft genome sequence of *Arthrobacter globiformis* mrc11, an antimicrobial agent isolated from a Khangkhui cave deposit. *Microbiol. Res. Announ.* **8** e01620-e11618

Saiki RK, Gelfand DH, Stoffel S, *et al*. 1988 Primer-directed enzymatic amplification of DNA with a thermostable DNA polymerase. *Science* **239** 487–491

Saitou N and Nei M 1987 The neighbor-joining method: a new method for reconstructing phylogenetic trees. *Mol. Biol. Evol.* **4** 406–425

Sanatombi K and Sharma GJ 2008 Capsaicin content and pungency of different *Capsicum* spp. cultivars. *Notulae Botanicae Horti Agrobotanici Cluj-Napoca* **36** 89–90

Schwyn B and Neilands JB 1987 Universal assay for the detection and determination of siderophores. *Anal. Biochem.* **160** 47–56

Song JY, Kim HA, Kim JS, Kim SY and Jeong H 2012 Genome sequence of the plant growth-promoting rhizobacterium *Bacillus* sp. strain JS. *J. Bacteriol.* **194** 3760–3761

Stephen FA, John CW, Michael GE, *et al*. 2005 Protein database searches using compositionally adjusted substitution matrices. *FEBS J.* **272** 5101–5109

Tamura K, Stecher G, Peterson D, Filipski A and Kumar S 2013 MEGA6: molecular evolutionary genetics analysis version 6.0. *Mol. Biol. Evol.* **30** 2725–2729

Tatusova T, DiCuccio M, Badretdin A, Chetvernin V and Nawrocki EP 2016 NCBI prokaryotic genome annotation pipeline. *Nucleic Acids Res.* **44** 6614–6624

Tilmann W, Kai B, Srikanth D, Daniel K and Hyun UK 2015 AntiSMASH 3.0—a Comprehensive resource for the genome mining of biosynthetic gene clusters. *Nucleic Acids Res*. https://doi.org/10.1093/nar/gkv437

Vanitha SC and Umesha S 2011 Pseudomonas fluorescens mediated systemic resistance in tomato is driven through an elevated synthesis of defense enzymes. *Biol. Plant.* **55** 317–322

Verma P, Yadav AN, Kazy SK, Saxena AK and Suman A 2014 Evaluating the diversity and phylogeny of plant growth-promoting bacteria associated with wheat (*Triticum aestivum*) growing in central zone of India. *Int. J. Curr. Microbiol. Appl. Sci.* **3** 432–447

Vessey JK 2003 Plant growth-promoting rhizobacteria as biofertilizers. *Plant Soil* **255** 571–586

Wang Y, Devin C-D, Chen G and Gu YQ 2015 OrthoVenn: a web server for genome wide comparison and annotation of orthologous clusters across multiple species. *Nucleic Acids Res.* **43** W78–W84

Wilson K 2001 Preparation of genomic DNA from bacteria. *Curr. Protoc. Mol Biol.* https://doi.org/10.1002/0471142727.mb0204s56

Wu GF, Wu XC, Xuan XD and Zhou XP 2006 Evaluation of nutrient limitation in aquatic ecosystems with nitrogen fixing bacteria. *J. Environ. Sci.* **18** 537–542

Xu H, Luo X, Qian J, *et al*. 2012 FastUniq: a fast de novo duplicates removal tool for paired short reads. *PLoS One* **7** e52249

Ye J, Fang L, Zheng H, *et al*. 2006 WEGO: a web tool for plotting GO annotations. *Nucleic Acids Res.* **34** 293–297

Zhang Z, Schwartz S, Wagner L and Miller W 2000 A greedy algorithm for aligning DNA sequences. *J. Comput. Biol.* **7** 203–214

Zhu C, Sun G, Chen X, Guo J and Xu M 2014 *Lysinibacillus varians* sp. nov., an endospore-forming bacterium with a filament-to-rod cell cycle. *Int. J. Syst. Evol. Microbiol.* **64** 3644–3649

Corresponding editor: Ashis Kumar Nandi